Hyperspectral response of wheat agronomic variables to background optical variability

Lin Gao[a], Roshanak Darvishzadeh[b], Ben Somers[c], Brian Alan Johnson[d], Yu Wang[e], Jochem Verrelst[f], Xiaofei Wang[a,*], Clement Atzberger[g]

[a] College of Geography and Environment, Shandong Normal University, Jinan 250014, China

[b] Faculty of Geo-Information Science and Earth Observation (ITC), University of Twente, P.O. Box 217, 7500 AE Enschede, the Netherlands

[c] Division Forest, Nature and Landscape, Department Earth and Environmental Sciences, KU Leuven, Leuven, Belgium, Celestijnenlaan 200E-2411, B-3001 Leuven, Belgium

[d] Institute for Global Environmental Strategies, Hayama, Kanagawa 240-0115, Japan

[e] School of Surveying and Land Information Engineering, Henan Polytechnic University, Jiaozuo 454000, China

[f] Image Processing Laboratory (IPL), Parc Científic, Universitat de València, 46980 Paterna, Spain

[g] Institute of Geomatics, University of Natural Resources and Life Sciences (BOKU), 1090 Vienna, Austria

Abstract

Understanding how biophysical and biochemical variables contribute to the spectral characteristics of vegetation canopies is critical for their monitoring. Quantifying these contributions, however, remains difficult due to extraneous factors such as the spectral variability of canopy background materials. Soil water content, soil type, and variable amounts of non-photosynthetic vegetation (NPV) are some of the factors that play a significant role in the spectral variability of the canopy background. This study focused on exploring the spectral response of two important agronomic variables (leaf chlorophyll content (C_{ab}) and leaf area index (LAI)) under various canopy backgrounds through global sensitivity analysis (GSA) algorithm for wheat canopy spectra simulated using the physically-based PROSAIL radiative transfer model. A quantitative investigation of the influence of the background on the spectral response of canopy to

C_{ab} and LAI reveals the following general findings: (1) the contribution of each agronomic variable to the simulated wheat canopy spectral signature varies considerably with respect to the background optical properties; (2) the influence of the background associated soil-type and NPV on the spectral response of canopy is more significant than that caused by background moisture; (3) individual spectral bands that are more sensitive to C_{ab} and much less affected by the impacts of variations in the NPV, soil-type and moisture are at 560 and 704 nm; (4) the near-infrared (NIR) spectral bands (774-900 nm) exhibit higher sensitivity to LAI over background soils with moisture than those differed in soil-type and NPV. Comparative analyses of the correlations of the twelve widely used vegetation indices further highlight the LICI (LAI-insensitive chlorophyll index), the Macc01 (Maccioni index), the OSAVI (optimized soil adjusted vegetation index) and the MCARI2 (modified chlorophyll absorption ratio index 2) are expected to provide critical information for C_{ab} and LAI estimation, respectively. Our results indicate that background reflectance variability contributes considerable differences in the spectral response of agronomic variables and thus would lead to the inconsistency of the VI- C_{ab} /-LAI relationship which naturally impedes their estimation accuracy from remote sensing measurements. Further studies would integrate these quantitative results of spectral responsivity to develop trait-specific hyperspectral inversion models.

1. Introduction

Plants are an essential component of the terrestrial ecosystem. Leaf area index (LAI), as an indicator of vegetation growth (Ma *et al.*, 2018), and the leaf chlorophyll content (C_{ab}), as an indicator of the photosynthetic capacity of vegetation (Croft *et al.*, 2017), are two of the most important vegetation variables that control water, energy and carbon exchange processes in the terrestrial biosphere. Knowledge of the spatial distribution of the LAI and C_{ab} is crucial to assess the terrestrial carbon and water balance and to forecast agricultural yield in the context of global changes (Chen *et al.*, 2019; Gitelson *et al.*, 2003; Houborg *et al.*, 2013; Huang *et al.*, 2015). Remote sensing

can provide such information by enabling the non-destructive estimation of LAI and C_{ab} at regional to global scales (Croft *et al.*, 2020; Fang *et al.*, 2019). The retrieval of LAI and C_{ab} from remote-sensing data relies on the fact that the optical properties of leaves and the canopy correlate strongly with vegetation amount and conditions (Asner 1998; Jacquemoud *et al.*, 2009). Consequently, an in-depth understanding of how the LAI and C_{ab} determine the vegetation spectral behavior including reflectance and vegetation indices (VIs), is vital for a more accurate estimation of LAI and C_{ab} from remote-sensing data.

Numerous studies have used simulations based on radiative transfer models to study the sensitivity of surface reflectance of a soil-vegetation system, usually through either global sensitivity analysis (GSA) or local sensitivity analysis (LSA) methods. The GSA quantifies the contribution of various model input parameters to the reflected electromagnetic radiation simultaneously (Gu *et al.*, 2016; Mousivand *et al.*, 2014; Wang *et al.*, 2019; Xiao *et al.*, 2014). In previous studies, however, GSA had ignored the fact that, even within a small agricultural field, the background optical properties generally vary spatially and temporally (Li *et al.* 1993). Such spatiotemporal variations in background reflectance are the main source of uncertainty in satellite-derived LAI or C_{ab} products (Darvishzadeh *et al.*, 2008; Darvishzadeh *et al.*, 2019; Eitel *et al.*, 2009; Verrelst *et al.* 2010). Conversely, the LSA is the qualitative analysis of the relationships between the spectral characteristics and a specific biophysical or biochemical parameter, while keeping the majority of the remaining variables fixed. This has been successfully applied to evaluate the spectral sensitivity of agronomic variables to different soil types and water contents (Bach and Verhoef, 2003; Díaz and Blackburn, 2003; Huete *et al.* 1985; Morcillo-Pallarés *et al.*, 2019). However, LSA cannot identify and quantify over the entire input variable space the influential and non-influential variables that govern the spectral signatures at different wavelengths (Saltelli and Annoni, 2010). Such assessments have important implications for selecting the optimal bands for the estimation of LAI and C_{ab}. Moreover, previous applications of LSA rarely focused on the spectral response in the shortwave infrared (SWIR) bands that are configured in popular satellite sensors (e.g., Landsat-8 OLI, Sentinel-2 MSI) and commonly used for

LAI retrievals (Amin *et al.*, 2021; Dong *et al.*, 2020).

To gain maximum understanding, sensitivity analyses should include major factors which contribute to the spectral variability of background materials. Typically, in many agricultural ecosystems, the background spectrum is highly heterogeneous due to different soil types/fertilizer treatments, non-photosynthetic vegetation (NPV, e.g., crop residue, litter, senescent grass), and seasonal surface water status. Therefore, it is imperative to elucidate the spectral response of vegetation variables under different background conditions. The two objectives of this study are: (1) to quantitatively investigate the contributions of LAI and C_{ab} to (i) the full-wavelength spectral response (400–2400 nm) and (ii) commonly available VIs when background optical properties are variable, and (2) to determine the spectral regions where the LAI and/or C_{ab} most strongly affect the canopy spectral characteristics while themselves being minimally influenced by variations in background reflectance. These research objectives are studied for a setting simulating wheat canopies (*Triticum aestivum* L.).

2. Materials and Methods

2.1. Background spectra

Mimicking vegetation spectra with variable backgrounds requires typical spectra from various background materials and appropriate canopy reflectance models. Spectral reflectance of various soil types in China were collected from (i) a subset of the ICRAF-ISRIC spectral library (the International Centre for Research in Agroforestry-International Soil Reference and Information Centre) as described by Garrity and Bindraban, 2004, and (ii) the CSSL spectral library (the Chinese Soil Spectral Library) described in Shi *et al.*, 2014. The ICRAF-ISRIC spectral library includes 245 soil profiles collected from 47 locations in China. The CSSL spectral library has 1581 soil samples derived from 16 soil groups of the Genetic Soil Classification of China. Fifty-one reflectance spectra of NPV were acquired from the ECOSTRESS spectral library (the ECOsystem Spaceborne Thermal Radiometer Experiment on Space Station, see Meerdink *et al.*, 2019 for details). To avoid data

redundancy caused by similar soil or NPV spectra in these three independent spectral libraries and to accelerate the simulations, we used the spectral angle mapping classification method (Kruse *et al.*, 1993) to identify several representative spectra based on the following equation:

$$\alpha_{XY} = \cos^{-1}\left[\frac{\sum_{i=1}^{n}(x_i y_i)}{\sqrt{(\sum_{i=1}^{n} x_i^2)} \times \sqrt{(\sum_{i=1}^{n} y_i^2)}}\right]$$

where, $X = (x_1, x_2, \ldots, x_n)$ and $Y = (y_1, y_2, \ldots, y_n)$ are two different soil spectral vectors with n wavebands; α_{XY} is the spectral angle between X and Y and ranges from 0 to π/2 (α_{XY} = 0 means that X and Y are completely similar, while α_{XY} = π/2 means that X and Y are entirely different).

Using the criterion that two different spectra with a spectral angle $\alpha < 0.05$ would be identified as similar reflectance (Jia et al., 2016), the spectral reflectance curves of 1826 soil and 51 NPV were classified into 17 soil and 24 NPV groups, respectively. In addition, a set of average spectra generated from a dataset containing 70 crop-residue and soil at seven moisture levels (Quemada and Daughtry, 2016) was used to mimic the canopy spectral variation due to differences in water contents of the ground underneath the canopy. In total, 55 different background reflectance were assessed (Figure 1): 17 soil types, 24 NPV, 7 soil moisture contents, and 7 crop-residue moisture contents. The chosen background spectra display distinct spectral contrast linked to soil type, composition, texture, and surface conditions, which permit to describe a wide range of natural backgrounds.

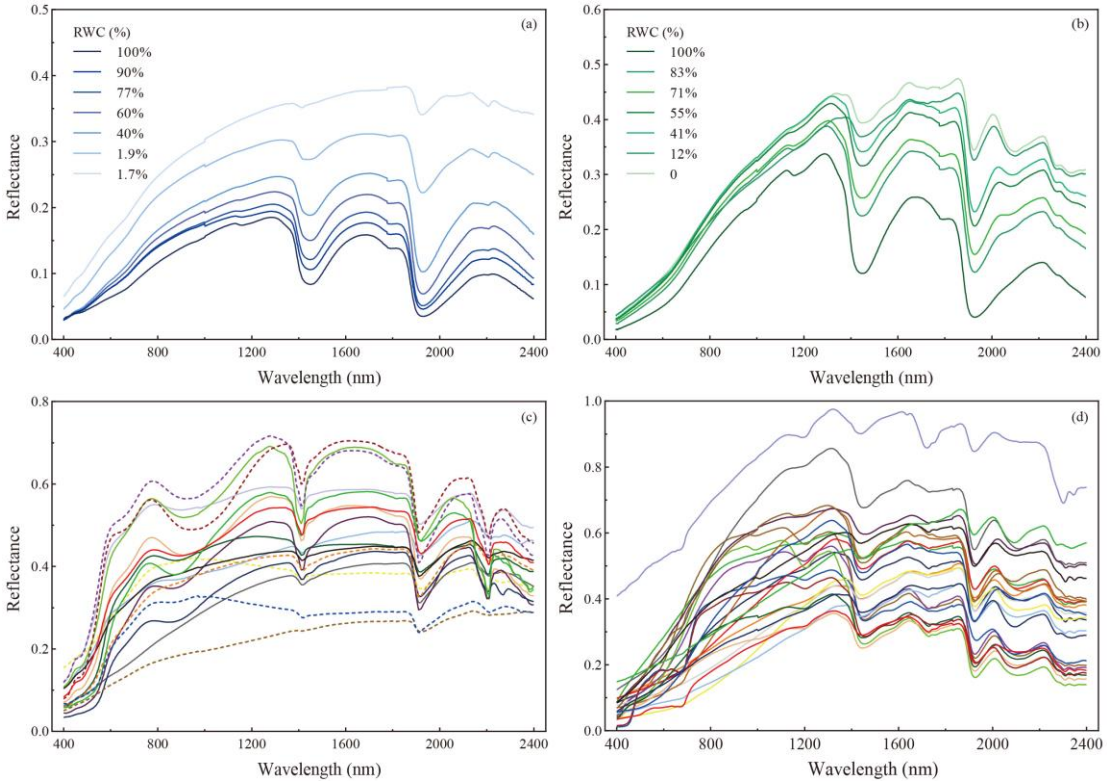


Figure 1. Reflectance spectra of various backgrounds used as input into the PROSAIL model: (a) bare soil at seven different relative water contents (RWC), (b) crop residue with seven different levels of moisture content, (c) 17 contrastive soil types, and (d) 24 NPV.

2.2. Global sensitivity analysis

We used the extended Fourier amplitude sensitivity test method (EFAST, Saltelli *et al*., 2008), implemented in the software package SimLab (ver. 2.2, SIMLAB, 2009) to perform the global sensitivity analysis of the simulated datasets. The EFAST is a variance-based GSA method, which has recently gained wider attention in agricultural modeling (Jin *et al*., 2018; Xu *et al*., 2019). The sensitivity measures of EFAST include the first-order sensitivity index S_i, which reflects the individual contribution of each input parameter to the model output, and the total-order sensitivity index ST_i, which represents the overall contribution of each parameter to the model output (including interactions between each parameter and the remaining parameters). Both sensitivity indices can be expressed as follow:

$$S_i = \frac{V_i}{V}$$

$$ST_i = S_i + \sum_{j \neq i} S_{ij} + \cdots + S_{1,2,\ldots,k}$$

where V_i ($V_i = V[E(Y|x_i)]$) represents the first-order variance for each input factor; V is the attribution of total output variance and calculated according to $V = \sum_{i=1}^{k} V_i + \sum_{i=1}^{k} \sum_{j>i}^{k} V_{ij} + \cdots + V_{1,2,\ldots,k}$; and V_{ij} ($V_{ij} = V\left[E(Y|x_i, x_j)\right] - V_i - V_j$) to $V_{1,2,\ldots,k}$ represent the interactions among k factors (see Saltelli *et al.*, 2010, for further details on EFAST).

The PROSAIL radiative transfer model (Jacquemoud *et al.*, 2009) was used to produce nadir-viewed wheat-like canopy reflectance (from 400 to 2400 nm in 1 nm increments), assuming negligible atmospheric effects. The MATLAB code for PROSAIL can be downloaded at http://teledetection.ipgp.jussieu.fr/prosail/. To better constrain and parameterize the PROSAIL model to simulate wheat spectral reflectance, specific ranges of the main model input variables were assigned based on information reported in prior studies or site-specific field campaigns (see Appendix A for details). Given that no fluctuations occur after 35 000 simulations per variable (see Appendix B), the total sample size of each input parameter of PROSAIL mode for EFAST was set to 40 000. These 40 000 parameter combinations were randomly generated within the predefined ranges by using EFAST, resulting in the generation of 40 000 canopy spectra by running PROSAIL in the forward mode. Then, the influence of the background on the contribution of C_{ab} and LAI to canopy reflectance as well as the twelve VIs selected (given in Appendix C) was examined by repeatedly running EFAST for each of the 55 background spectra (i.e., 7 soil moisture contents, 7 crop-residue moisture contents, 17 soil types, and 24 NPV types). Furthermore, for comparison between the spectral response of the canopy with the background and that with a non-reflecting background (assumed to be background-free interference), "pure" vegetation spectra were also generated by inserting "zero" for background reflectance in the simulation of each band (Jean-Baptiste Feret, personal communication; Gao *et al.*, 2000), equivalent to the canopy bounded at below by a fully absorbing background

(Shabanov *et al.*, 2000). The global sensitivity of pure vegetation spectra, as well as their VIs (termed "pure" VI hereafter), was then calculated.

3. Results and Discussion

3.1. Global sensitivity analysis results of canopy spectra with fully absorbing background

A few studies have discussed the results of the GSA in PROSAIL based on one specific soil background (e.g., Xiao *et al.* 2014; Verrelst *et al.*, 2016); hence this scenario is not considered herein. Instead, Figure 2 gives the background-free (totally absorbing) results of the GSA. The results for S_i reveal that the contributions of the inputs to the plant-canopy spectra depend on wavelength and differ considerably from that of the background scenarios.

LAI and average leaf inclination angle (ALA) are responsible for about 20% and 73%, respectively, of the canopy reflectance variability in the wavelength range 400–500 nm. C_{ab} is the main driver of the canopy reflectance variability in the wavelength range 500–720 nm, explaining about 0%–65% of the variation, but beyond about 720 nm its contribution gradually disappears caused by the fact that C_{ab} is transparent to infrared radiation (Verrelst *et al.* 2015). The contribution of C_{ab} peaks at roughly 585 and 695 nm. In the NIR wavelength range of 720–1300 nm, the canopy reflectance variation is controlled primarily by ALA, LAI, and dry matter content (C_m), which account for roughly 28%–35%, 20%–41%, and 4%–22% of the variation, respectively. Despite negligible influence on the spectra in the visible and near-infrared (VNIR) region, equivalent water thickness (C_w) explains about 10%–61% of the canopy reflectance variation in the SWIR wavelength range of 1300–2400 nm, especially for wavelengths longer than 1880 nm (termed "SWIR2" hereafter) with a contribution of 31%–61%. In contrast, LAI drives less than 12% to variations in SWIR2 reflectance. This finding is contrary to that of Xiao *et al.* (2014) and Verrelst *et al.* (2015) who found that LAI governed over 50% of the variation in SWIR2 reflectance greater than C_w does in the background cases. This inconsistency is tentatively attributed to the fact that the

background has a much higher single-scattering albedo in the SWIR2 spectral part than does green vegetation, so the SWIR2 reflectance of plant canopy mixed with the background is more sensitive to changes in the LAI than that under the zero-background case in the absence of specular reflection. As can be seen in Figure 2, the remaining variables leaf structure parameter (N) and solar zenith angle (θ_s) only slightly impact the reflectance over the entire spectral range (together, <14%).

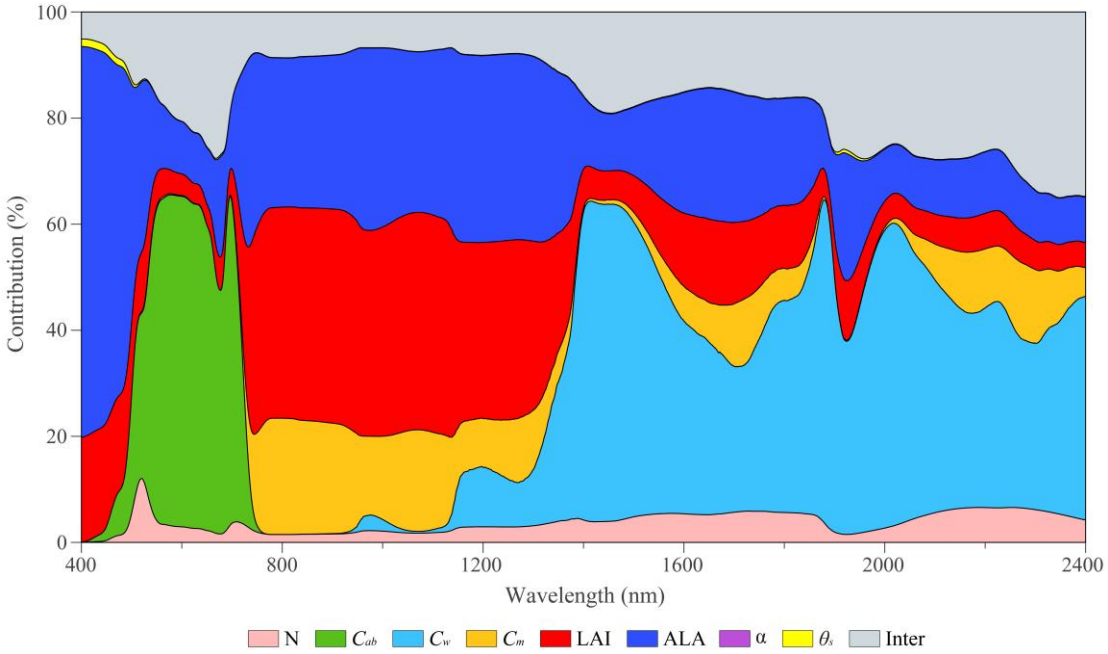


Figure 2. Main effect and interactions of the EFAST sensitivity analysis on vegetation biophysical and biochemical parameters with a totally absorbing background.

3.2. Variations in chlorophyll- or LAI-related spectral response with various background cases

3.2.1 Sensitivities of spectral signatures

To avoid duplicating efforts for the qualitative assessment of the sensitivity of wheat reflectance to soil background in the VNIR region, we quantify how much the background reflectance differences-induced changes in the spectral response of the LAI and C_{ab} over background scenarios based on the mean and the standard deviation (sd) of the S_i as the criterion in this article (see Figures 3). Differences in S_i at a certain wavelength (as displayed by sd) reveal how much the contribution of the C_{ab} to wheat

canopy reflectance varies owing to background variability (see Figure 3a and the S_i of canopy reflectance beyond 800 nm not shown in figures). Although wheat canopy reflectance around 530–590 nm and around 690–710 nm is more sensitive to C_{ab} than in other spectral regions, the sensitive peaks within both regions are closely correlated with the background, which is little known in the literature: the sensitive peaks are near 560 and 704 nm for variations in soil type, near 570 and 700 nm for NPV, and near 595 and 696 nm for variations in soil or crop-residue moisture content. Nevertheless, the impact of variations in backgrounds on canopy reflectance at 560 and 704 nm response to C_{ab} is relatively less than whose impact on other peak positions. Thus, the use of canopy reflectance at 560 and 704 nm as predictors of C_{ab} estimates is desirable. This finding provides powerful support for spatially explicit monitoring of chlorophyll content using the Sentinel-2 data, which have green and red-edge bands with center wavelengths of 560 and 704 nm, respectively. Furthermore, the canopy reflectance around 680 nm, which matches the chlorophyll absorption peaks, is closely related to C_{ab} only when including variations in background moisture but is less sensitive to C_{ab} when including variations in soil type. Importantly, the sensitivity of canopy reflectance around 680 nm decreases with increasing background moisture. These results obtained in the context of variations in background reflectance thus seem to contradict earlier findings by Verrelst *et al.* (2016) that suggest that C_{ab} is reasonably well correlated with reflectance at 500, 564, 710, and 714 nm in a scenario with a single soil type.

Furthermore, the impacts of background spectral properties on the response of canopy reflectance to changes in LAI are quite different for different spectral regions. As shown in Figure 3b, spectral variations associated with soil-type and NPV affect the LAI-related spectral response of the spectral windows 450–528 and 633–691 nm more than does soil or crop-residue moisture, especially at the pigment-absorption features (around 487 and 675 nm). For instance, LAI explains 28% ± 18% and 44% ± 12% (when varying soil types) and 26% ± 16% and 30% ± 16% (when varying NPV) of variations in canopy reflectance at 487 and 675 nm, respectively, as opposed to 5% ± 10% and 10% ± 10% (when varying soil moisture) and 3% ± 3% and 13% ± 5% (when varying crop-residue moisture), respectively. Interestingly, the wheat reflectance

spectrum response in the NIR range (774–900 nm) to LAI over background cases of soil-type and NPV is less than the response with a wet background. Although the former imposes a greater influence on spectral sensitivity (> ±8%) than the latter (approximately ±3%). In contrast, in the range 1900–2400 nm, differences in soil or crop-residue moisture affect the spectral response to LAI more than differences in soil types do, particularly at water absorption features (around 1930 nm).

These discrepancies in the response of canopy reflectance to LAI or C_{ab} can render wavelength selection a substantial challenge. Although the "lambda-by-lambda" band-optimization algorithm suggested by Yu *et al.* (2014) could determine the sensitive bands, it is suitable merely for field-scale measurements and not for large-scale monitoring. In contrast, spectral-band selection using Gaussian process regression (Verrelst *et al.*, 2016), random forest regression (Liu *et al.*, 2019), and even multi-method ensembles consisting of partial least squares, random forest, and support vector machine regression (Feilhauer *et al.*, 2015) seem more appropriate because of its powerful capacity for band-ranking features over very large datasets. Unfortunately, previous band-selection experiments have been little concerned about the variations in the spectral response of canopy with different backgrounds. In future research, the spectral behavior of the canopy with various backgrounds such as those given here may serve as a *prior* knowledge to select an optimal set of spectral bands and thus improve the estimation of LAI and C_{ab} particularly with spectral mixture analysis (e.g., Tits *et al.*, 2013).

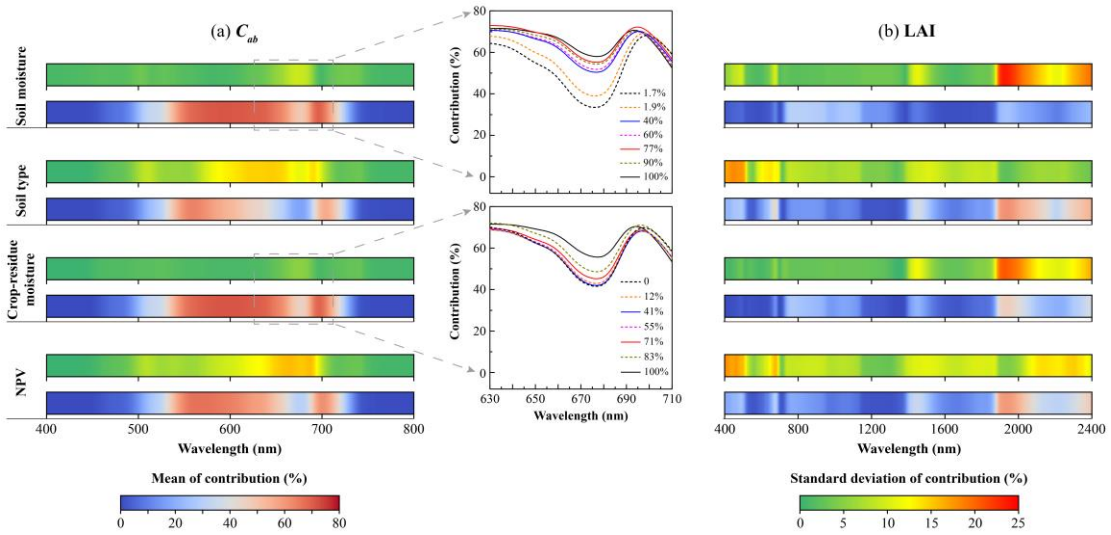


Figure 3. The first-order sensitivity indices with associated error (mean ± standard deviation) of hyperspectral reflectance to C_{ab} (a) and LAI (b) over different background scenarios including soil-type, soil moisture, NPV, and crop-residue moisture.

3.2.2 Sensitivities and correlations of VIs -C_{ab} and -LAI

Another problem requiring attention involves variations in the response of VIs that are extensively applied in the large-scale retrieval of LAI or C_{ab}, to background variations. The response of the VIs to variation in C_{ab} or LAI and the correlations between agronomic variables and the VIs using simulations performed with all scenarios (described in Section 2.2) are illustrated in Figure 4. In general, there are obviously some variability in the S_i and the coefficient of determination (R^2) of the chlorophyll-related indices caused by variations in background spectral properties, especially associated with soil type and NPV. The effect of background moisture status on the C_{ab}-VIs relationships is minor, since the spectral bands employed in these chlorophyll-related indices are less affected by background moisture (see Figure 3a). The photochemical reflectance index (PRI) remains highly sensitive to C_{ab} for all backgrounds except soil type resulting in considerable differences in its responsiveness (with a larger interquartile range of S_i, IQR of 13%). The worst C_{ab}-PRI relationships are obtained in background cases of soil types with R^2 of 0.59 ± 0.07 (mean ± sd). This implies that PRI is susceptible to variations in soil background, which is consistent with the earlier discussion of Barton and North (2001). Thus, caution is warranted when

determining the light-use efficiency based on satellite-derived PRI over large geographic regions with contrasting soil types. By contrast, Macc01 and LICI are superior to PRI for extracting chlorophyll content, as evidenced by the relatively higher sensitivity (S_i > 79% on average individually) and better relationships with C_{ab} (R^2 > 0.75 on average individually). Variability of the R^2 values concerning changes in background reflectance also indicates that both indices are more strongly resistant to background effects. In theory, the LICI was recognized to be independent of LAI (Li *et al.*, 2020) with only a marginal S_i (< 2%) and hence is the most robust chlorophyll-related index of the VIs tested here (i.e., considering both background and canopy structure effects). In contrast with other chlorophyll-related indices, the red-edge-based spectral indices such as the red-edge chlorophyll index (CI_{RE}) and MCARI/OSAVI$_{(705, 750)}$ are less sensitive to changes in chlorophyll content, although both indices are reported to be more closely related to chlorophyll content than their original versions (Gitelson *et al.*, 2005; Wu *et al.*, 2008). Nonetheless, the sensitivity of MCARI/OSAVI$_{(705, 750)}$ to C_{ab} is very little affected by variability in background reflectance, as evinced by low values of the standard deviation of R^2 (with sd < 0.01), because the OSAVI-based 705 nm feature is integrated to mitigate the effect of soil and NPV. Overall, these commonly used chlorophyll-related indices differ in their responses and they may resist the effect of background to some extent. Compared with the chlorophyll-related indices, background optical variability does more strongly influence the GSA and correlation results of the LAI-related indices. More importantly, the impact of NPV on the response of the LAI-related indices to LAI is more significant than those on the response of the chlorophyll-related indices to C_{ab}. The NDVI (normalized difference vegetation index) is subject to variability associated with soil brightness (Huete, 1988; Huete & Tucker, 1991). The sensitivity of the NDVI to LAI thus shows variability due to soil or crop-residue moisture. The spectral influence of soil type and NPV, aside from brightness, cause more differences in the S_i of NDVI (with IQR of about 8% on average individually). Moreover, the NDVI-LAI relationship is found to be poor (R^2 varied from 0.2 to 0.4 for canopy backgrounds). These outcomes partly explain the inconsistency of the NDVI-LAI relationships between remote-

sensing pixels that thus leads to substantial uncertainty associated with LAI estimates, especially for seasonal crop growth monitoring at the global scales (Liu *et al*., 2012; Liu & Huete, 1995; Xu *et al*., 2020). Similarly, there are also considerable variations in the responsiveness of MSR to LAI, especially over NPV (with IQR of 6.8%), because the sensitivity of individual spectral bands (i.e., red and NIR) varies strongly with spectral variability of non-photosynthetic materials (see Figure 3b). A recent study by Dong *et al*. (2019) recommended the substitution of the red reflectance by the red-edge reflectance (e.g., in the 690-730 nm region), to develop the red-edge MSR as a better crop LAI estimator. In contrast, MCARI2 could more effectively measure the canopy LAI than NDVI and MSR because it shows a relatively stable response to LAI over soil backgrounds (with rather small IQR, < 1.5%) and less susceptibility to chlorophyll concentration (with S_i < 2%). These results corroborate the well-established idea that MCARI2 is a significant improvement in monitoring crop LAI for precision agriculture (Haboudane *et al.* 2004). However, MCARI2 exhibits a notable discrepancy in the correlations with LAI(as evinced by R^2 with 0.34 ± 0.02) due to the presence of NPV. It might indicate that MCARI2 is more appropriate for remote sensing estimation of LAI in soil background than in situations where NPV is a significant component of surface cover. While early studies inherently disregard the occurrence of non-photosynthetic materials -particularly the appreciable amounts of woody stems and standing litter present in no-tillage fields. More fieldwork on the effects of NPV on MCARI2 representing vegetation activity (e.g., LAI) is needed in agricultural applications. The standardized LAI Determining Index (sLAIDI) is almost insensitive to variations in chlorophyll content (with minimal S_i, < 0.01%) that is in agreement with the results reported by Delalieux *et al.* (2008) who proposed sLAIDI for LAI estimation without the interference of chlorophyll effects. Contrary to expectations, however, the sLAIDI exhibits poor correlations with LAI, particularly across various soil types and NPV (with R^2 of 0.26 ± 0.06 on average individually).

Furthermore, in comparison with LAI-related indices, soil-corrected VIs such as OSAVI and MSAVI respond to LAI with minimal interference of background moisture (this is especially the case for the OSAVI with relatively higher sensitivity, as evinced

by the median of S_i with about 52% and IQR of about 1%). In addition, only OSAVI out of the 10 VIs shows stronger correlations with LAI over soil-type background (R^2 of 0.36 ± 0.004). However, there are relatively large discrepancies in the relationships between LAI and OSAVI and MSAVI in the sites consisting almost entirely of NPV, as confirmed by larger deviations in R^2 (with sd = 0.2 and 0.3, respectively). Prior studies (e.g., Li *et al*., 2019) mostly focused on the evaluation of soil brightness and saturation effects for estimating LAI using soil-corrected VIs. There is as yet a dearth of knowledge about the soil-corrected VIs related spectral behavior to LAI in the areas with abundant non-photosynthetic materials which is present in most semi-arid landscapes. These findings imply that, regardless of the robustness of these indices based on the soil line concept (Baret *et al*., 1993), background effects of soil-type, as well as NPV, cannot be removed entirely. Based on our findings, main discrepancies on the relationship of spectral characteristics and the LAI are easily occurred in agricultural land with contrastive soil types and NPV rather than in which with different moisture contents, mainly due to the former resulting substantial variations in LAI-related spectral response. Consequently, new VI-correction methods have been proposed based on the fraction of canopy cover to mitigate the background effects (Li *et al*., 2016; Van Beek *et al*., 2015; Yao *et al*., 2014).

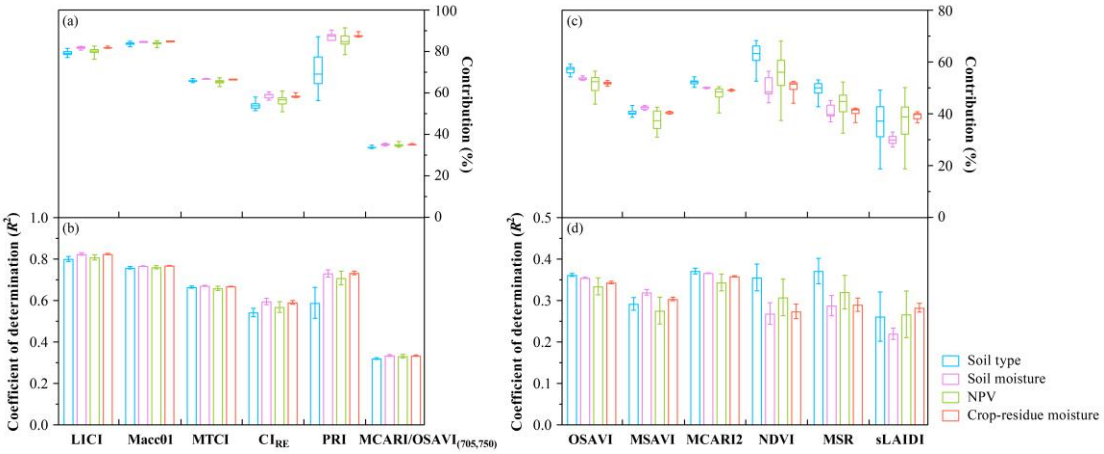


Figure 4. The first-order sensitivity indices as measures of the VIs response to C_{ab} (a) and LAI (c) using global sensitivity analysis and the coefficient of determination (R^2) for the relationships between VIs and C_{ab} (b) and LAI (d) based on the synthetic datasets.

For each VI, the boxplot was calculated by S_i; the mean and standard deviation were derived from R^2 values across different background scenarios (17 soil types, 7 soil moisture contents, 24 NPV, and 7 crop-residue moisture contents).

3.3. Comparison of the spectral response of canopy with and without background

The influence of the background on the spectral response of canopy was further examined by comparison to whose responsiveness with a fully absorbing background. Surprisingly, the S_i of canopy reflectance in the 550-710 nm range to C_{ab} (see Figure 3a) is larger with a wet background and is lower with contrastive soil-type where results are compared to those S_i with completely absorbing background (see Figure 2). In this spectral range, the chlorophyll sensitivity peak of canopy spectra is observed to have a "blue shift" (towards shorter wavelengths) due to background variability associated with soil-type and NPV, whereas the peak is detected as a "redshift" (towards longer wavelengths) because of background variations linked to moisture contents, in contrast with the highest sensitivity occurred at 585 nm with a fully absorbing background. Moreover, only in the cases of soil-type and NPV does the chlorophyll sensitivity peak in the red-edge range of 690 to 730 nm shift toward longer wavelength, as compared to its peak at 696 nm with fully absorbing background. Besides, Figure 2 and 3b reveals that the sensitivity of canopy spectra in the NIR plateau (800–1300 nm) to LAI decreases dramatically while the sensitivity of red reflectance in the wavelength interval [665, 680 nm] and SWIR2 reflectance increases compared to those responsiveness in a totally absorbing background, respectively.

Furthermore, the comparison of the response of VIs over canopy backgrounds with their "pure" counterparts responsiveness under fully absorbing background (as presented in Figure 5) illustrates the performance of the VIs (especially LAI-related indices) could be misleading due to background optical properties. The sensitivity of NDVI to LAI in the zero-background case (S_i = 7%) is far less than that with canopy backgrounds. Theoretically, the NDVI lies with the spectral contrast between red and NIR signatures (Rahman *et al*., 2004). The NDVI-LAI insensitivity can be accounted for by the fact that the red-NIR contrast is fairly uniform under a 100% absorbing

background due to multiple interactions within the canopy only, which is similar to the saturation of NDVI at high values of LAI. This result is in agreement with the findings of Gao *et al.* (2000). While the multiple scattering process in the vegetation background theoretically enhances the response of NDVI to LAI changes and thus the NDVI-LAI relationship has a larger correlation coefficient than that under totally absorbing background (R^2 = 0.04). Likewise, the sensitivities and correlations of MSR-LAI and sLAIDI-LAI relationships are found to be larger than that with totally absorbing background (S_i = 12% and 14%, R^2 = 0.09 and 0.11, respectively). Note that this positive contribution of canopy background to spectral response of VIs only is observed for LAI-related VIs including NDVI, MSR, and sLAIDI responsiveness to LAI but are rarely found in VIs related to chlorophyll content. In addition, the response of MCARI/OSAVI$_{(705, 750)}$ to LAI although less than that to C_{ab} is little variation across different canopy backgrounds comparable to that with fully absorbing background (S_i = 22%, R^2 = 0.2).

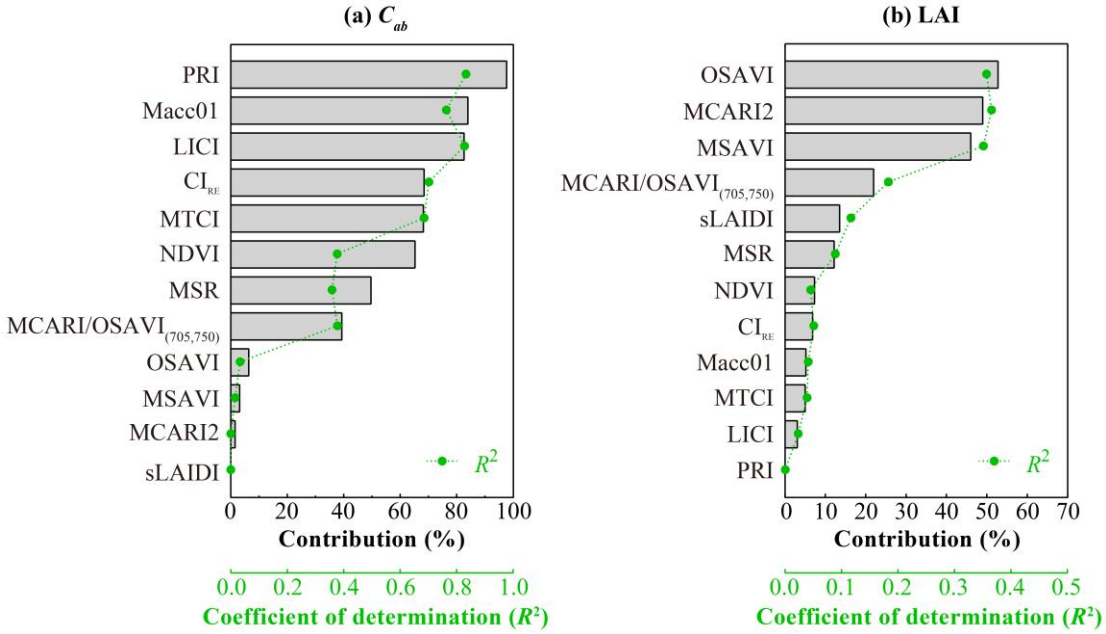


Figure 5. Sensitivity and correlation of VI to C_{ab} (a) and LAI (b) with completely absorbing background

4. Conclusions

Unraveling the spectral response of agronomic variables over different

backgrounds is of fundamental importance for effective monitoring of crop physiological and phenological status via remotely sensed data. This work quantifies the sensitivities of spectral reflectance and VIs to two agronomic variables (i.e., the C_{ab} and LAI) with various canopy backgrounds using an EFAST with PROSAIL simulations. The contribution of each parameter to the spectral behavior of wheat-like canopies varies with backgrounds, particularly associated with soil-type and NPV whose impacts are more significant than that caused by background moisture. In terms of hyperspectral band selection for remotely-sensed chlorophyll content estimates, our analysis suggests that the canopy reflectance at 560 and 704 nm are desirable due to both with relatively high sensitivity and soil-noise resistance. Besides, the canopy spectra in the interval 774–900 nm although those have been widely acknowledged as an essential part of deriving LAI exhibit robust spectral response to LAI only for wet background surfaces, while its sensitivity to LAI shows remarkable differences among cases of background soil-type and NPV. Furthermore, comparing analyses of the sensitivities and correlations of VI -C_{ab}/LAI between canopy backgrounds demonstrate that background reflectance variability is a critical factor leading to uncertainty in the estimation of C_{ab} and LAI using satellite data. Our analysis points out that the LICI, Macc01 and OSAVI, MCARI2 would provide better estimates of C_{ab} and LAI, respectively, because of those more responsiveness and better correction of background influences. In addition, an area-wide canopy background classification based on *a priori* knowledge of landscape stratification is indispensable for mapping large-scale chlorophyll content and LAI of wheat at a regional scale.

Although the analysis presented here is from simulated data, model simulations are essential to gain an adequate understanding of the spectral response of biophysical and biochemical parameters with different canopy backgrounds, which is not easily available from measurements and observations in the field and/or laboratory. Furthermore, these results are also applicable to other plant types that are structurally similar to wheat. More importantly, our findings help to improve understanding of the subtle changes in the relationships between hyperspectral features and C_{ab} and LAI over various background scenarios, which is one of the fundamental mechanisms for their

retrieval via the current generation of hyperspectral satellite sensors (e.g., GF-5/AHSI, PRISMA), and those anticipated in the near future (e.g., EnMAP, CHIME, HISUI), and is thus pivotal for accurately diagnosing crop growth status.

Acknowledgement

This research was partly supported by the National Natural Science Foundation of China (No. 42101334, 42101335), and the Natural Science Foundation of Shandong Province (No. ZR2021QD120, ZR2021QD015, ZR2020QD011). The first author especially acknowledges the tremendous amount of feedback of Dr. Jin Xu which has greatly improved the paper.

References

Amin E., Verrelst J., Rivera-Caicedo J. P., Pipia L., Ruiz-Verdú A., Moreno J. (2021). Prototyping Sentinel-2 green LAI and brown LAI products for cropland monitoring. *Remote Sensing of Environment*, 255, 112168.
https://doi.org/10.1016/j.rse.2020.112168

Asner, G. P. (1998). Biophysical and biochemical sources of variability in canopy reflectance. *Remote Sensing of Environment,* 64 (3), 234-253.
https://doi.org/10.1016/S0034-4257(98)00014-5

Bach, H., & Verhoef, W. (2003). Sensitivity studies on the effect of surface soil moisture on canopy reflectance using the radiative transfer model GeoSAIL. *IEEE International Geoscience and Remote Sensing Symposium*. *Proceedings*. IEEE, 3, 1679-1681.
https://dio.org/ 10.1109/IGARSS.2003.1294215

Baret, F., Jacquemoud, S., & Hanocq, J. F. (1993). The soil line concept in remote sensing. *Remote Sensing Reviews*, 7, 65-82.
https://doi.org/10.1080/02757259309532166

Barton, C.V.M., & North, P.R.J. (2001). Remote sensing of canopy light use efficiency using the photochemical reflectance index Model and sensitivity analysis. *Remote Sensing of Environment*, 78, 264-273. https://doi.org/10.1016/S0034-4257(01)00224-3

Chen, J.M. (1996). Evaluation of vegetation indices and a modified simple ratio for boreal applications. *Canadian Journal of Remote Sensing*, 22, 229-242. https://doi.org/10.1080/07038992.1996.10855178

Chen, J. M., Ju, W., Ciais, P., Viovy, N., Liu, R., Liu, Y., & Lu, X. (2019). Vegetation structural change since 1981 significantly enhanced the terrestrial carbon sink. *Nature Communications*, 10, 4259. https://doi.org/10.1038/s41467-019-12257-8

Croft, H., Chen, J. M., Luo, X., Ba Rtlett, P., Chen, B., & Staebler, R. M. (2017). Leaf chlorophyll content as a proxy for leaf photosynthetic capacity. *Global Change Biology*, 23, 3513-3524. https://doi: 10.1111/gcb.13599

Croft, H., Chen, J. M., Wang, R., Mo, G., Luo, S., Luo, X., *et al.* (2020). The global distribution of leaf chlorophyll content. *Remote Sensing of Environment*, 236, 111479. https://doi.org/10.1016/j.rse.2019.111479

Darvishzadeh, R., Skidmore, A., Atzberger, C., & Wieren, S. (2008). Estimation of vegetation LAI from hyperspectral reflectance data: Effects of soil types and plant architecture. *International Journal of Applied Earth Observation and Geoinformation*, 10, 358-373. https://doi.org/10.1016/j.jag.2008.02.005

Darvishzadeh, R., Skidmore, A., Abdullah, H., Cherenet, E., Ali A., Wang, T., *et al*. (2019). Mapping leaf chlorophyll content from Sentinel-2 and RapidEye data in spruce stands using the invertible forest reflectance model. *International Journal of Applied Earth Observation and Geoinformation*, 79, 58-70. https://doi.org/10.1016/j.jag.2019.03.003

Dash, J., & Curran, P. J. (2004). The MERIS terrestrial chlorophyll index. *International Journal of Remote Sensing*, 25, 5403-5413. https://doi.org/10.1080/0143116042000274015

Delalieux, S., Somers, B., Hereijgers, S., Verstraeten, W. W., Keulemans, W., & Coppin, P. (2008). A near-infrared narrow-waveband ratio to determine leaf area index in orchards. *Remote Sensing of Environment*, 112, 3762-3772. https://doi.org/10.1016/j.rse.2008.05.003

Díaz, B. M., & Blackburn, G. A. (2003). Remote sensing of mangrove biophysical

properties: Evidence from a laboratory simulation of the possible effects of background variation on spectral vegetation indices. *International Journal of Remote Sensing*, 24(1), 53-73. https://doi.org/10.1080/01431160305012

Dong, T., Liu, J., Shang, J., Qian, B., He L., Liu J., *et al.* (2020). Estimating crop biomass using leaf area index derived from Landsat 8 and Sentinel-2 data. *ISPRS Journal of Photogrammetry and Remote Sensing*, 168, 236-250. https://doi.org/10.1016/j.isprsjprs.2020.08.003

Dong, T., Liu, J., Shang, J., Qian, B., Ma, B., Kovacs, J. M. *et al*. (2019). Assessment of red-edge vegetation indices for crop leaf area index estimation. *Remote Sensing of Environment*, 222, 133-143. https://doi.org/10.1016/j.rse.2018.12.032

Eitel, J., Long, D. S., Gessler, P. E., Hunt, E. R., & Brown, D. J. (2009). Sensitivity of ground-based remote sensing estimates of winter chlorophyll content to variation in soil reflectance. *Soil Science Society of America Journal*, 73, 1715-1723. https://doi.org/10.2136/sssaj2008.0288

Fang, H., Baret, F., Plummer, S., & G Schaepman-Strub. (2019). An overview of global leaf area index (LAI): Methods, products, validation, and applications. *Reviews of Geophysics*. 57. https://doi.org/10.1029/2018RG000608

Feihauer, H., Asner, G. P., & Martin, R. E. (2015). Multi-method ensemble selection of spectral bands related to leaf biochemistry. *Remote Sensing of Environment*, 164, 57-65. https://doi.org/10.1016/j.rse.2015.03.033

Feret, J. B., François, C., Gitelson, A., Asner, G. P., Barry, K. M., Panigada C., *et al.* (2011). Optimizing spectral indices and chemometric analysis of leaf chemical properties using radiative transfer modeling. *Remote Sensing of Environment*, 115, 2742-2750. https://doi.org/10.1016/j.rse.2011.06.016

Gamon, J. A., Peñuelas, J., & Field, C. B. (1992). A narrow-waveband spectral index that tracks diurnal changes in photosynthetic efficiency. *Remote Sensing of Environment*, 41, 35-44. https://doi.org/10.1016/0034-4257(92)90059-S

Gao, X., Huete, A. R., Ni, W., & Miura, T. (2000). Optical-biophysical relationships of

vegetation spectra without background contamination. *Remote Sensing of Environment*, 74, 609-620. https://doi.org/10.1016/S0034-4257(00)00150-4

Garrity, D., & Bindraban, P. (2004). A globally distributed soil spectral library visible near infrared diffuse reflectance spectra. *ICRAF (World Agroforestry Centre)/ISRIC (World Soil Information) Spectral Library: Nairobi, Kenya*.

Gitelson, A. A., Keydan, G. P., Merzlyak M. (2006). Three-band model for noninvasive estimation of chlorophyll, carotenoids, and anthocyanin contents in higher plant leaves. *Geophysical Research Letters*, 33, L11402. https://doi.org/10.1029/2006GL026457

Gitelson, A. A., Viña, A., Arkebauer, T. J., Rundquist, D. C., Keydan, G., Leavitt, B. (2003). Remote estimation of leaf area index and green leaf biomass in maize canopies. *Geophysical Research Letters*, 30, 1248. https://doi.org/10.1029/2002GL016450

Gitelson, A. A., Viña, A., Ciganda, V., Rundquist, D., Arkebauer, T. J. (2005). Remote estimation of canopy chlorophyll content in crops. *Geophysical Research Letters*, 32, L08403. https://doi.org/10.1029/2005GL022688

Gu, C., Du, H., Mao, F., Han, N., Zhou, G., Xu, X., *et al.*, (2016). Global sensitivity analysis of PROSAIL model parameters when simulating Moso bamboo forest canopy reflectance. *International Journal of Remote Sensing*, 37, 5270-5286. https://doi.org/10.1080/01431161.2016.1239287

Haboudane, D., Miller, J. R., Pattey, E., Zarco-Tejada, P. J., & Strachan, I. B. (2004). Hyperspectral vegetation indices and novel algorithms for predicting green LAI of crop canopies: Modeling and validation in the context of precision agriculture. *Remote Sensing of Environment*, 90, 337-352. https://doi.org/10.1016/j.rse.2003.12.013

Houborg, R., Cescatti, A., Migliavacca, M., & Kustas, W. P. (2013). Satellite retrievals of leaf chlorophyll and photosynthetic capacity for improved modeling of GPP. *Agricultural and Forest Meteorology*, 177, 10-23. https://doi.org/10.1016/j.agrformet.2013.04.006

Huang, J., Tian, L., Liang, S., Ma, H., Becker-Reshef, I., Huang, Y., et al. (2015). Improving winter wheat yield estimation by assimilation of the leaf area index from Landsat TM and MODIS data into the WOFOST model. *Agricultural and Forest Meteorology*, 204, 106-121. https://doi.org/10.1016/j.agrformet.2015.02.001

Huete, A. R. (1988). A soil adjusted vegetation index (SAVI). *Remote Sensing of Environment*, 25, 295-309. https://doi.org/10.1016/0034-4257(88)90106-X

Huete, A. R., Jackson, R. D., & Post, D. F. (1985). Spectral response of a plant canopy with different soil background. *Remote Sensing of Environment*, 17(1), 37-53. https://doi.org/10.1016/0034-4257(85)90111-7

Huete, A. R., & Tucker, C. J. (1991). Investigation of soil influences in AVHRR red and near-infrared vegetation index imagery. International Journal of Remote Sensing, 12(6), 1223-1242. https://doi.org/10.1080/01431169108929723

Jacquemoud, S., Verhoef, W., Baret, F., Bacour, C., Zarco-Tejada, P. J., Asner, G. P., *et al.* (2009). PROSPECT+SAIL models: A review of use of vegetation characterization. *Remote Sensing of Environment*, 113, S56-S66. https://doi.org/10.1016/j.rse.2008.01.026

Jia, K., Liang, S., Gu, X., Baret, F., Wei, X., Wang, X., *et al*. (2016). Fractional vegetation cover estimation algorithm for Chinese GF-1 wide field view data. *Remote Sensing of Environment*, 177, 184-191. http://dx.doi.org/10.1016/j.rse.2016.02.019

Jin, X., Li, Z., Nie, C., Xu, X., Feng, H., Guo, W., & Wang, J. (2018). Parameter sensitivity analysis of the AquaCrop model based on extended fourier amplitude sensitivity under different agro-meteorological conditions and application. *Field Crops Research*, 226, 1-15. https://doi.org/10.1016/j.fcr.2018.07.002

Kruse, F. A., Lefkoff, A. B., Boardman, J. W., Heidebrecht, K. B., Shapiro, A. T., Barloon, P. J., & Goetz, A. F. H. (1993). The spectral image processing system (SIPS)—Interactive visualization and analysis of imaging spectrometer data. *Remote Sensing of Environment*, 44, 145-163. https://doi.org/10.1016/0034-4257(93)90013-N

Li, D., Chen, J. M., Zhang, X., Yan, Y., Zhu, J., Zheng, H., *et al.* (2020). Improved estimation of leaf chlorophyll content of row crops from canopy reflectance spectra through minimizing canopy structural effects and optimizing off-noon observation time. *Remote Sensing of Environment*, 248, 111985. https://doi.org/10.1016/j.rse.2020.111985

Li, F., Zeng, Y., Luo, J., Ma, R., & Wu, B. (2016) Modeling grassland aboveground biomass using a pure vegetation index. *Ecological Indicators*, 62, 279-288.

https://doi.org/10.1016/j.ecolind.2015.11.005

Li, H., Coburn, C. A., Wang, Z. J., Wei, F., & Guo, T. C. (2019). Reduced prediction saturation and view effects for estimating the leaf area index of winter wheat. *IEEE Transactions on Geoscience and Remote Sensing*, 57, 1637-1652. https://doi.org/10.1109/TGRS.2018.2868138

Li, Y., Demetriades-Shah, T. H., Kanemasu, E. T., Shultis, J. K., & Kirkham, M. B. (1993). Use of second derivatives of canopy reflectance for monitoring prairie vegetation over different soil background. *Remote Sensing of Environment*, 44(1), 81-87. https://doi.org/10.1016/0034-4257(93)90104-6

Liang, L., Di, L., Zhang, L., Deng, M., Qin, Z., Zhao, S., & Lin, H. (2015). Estimation of crop LAI using hyperspectral vegetation indices and a hybrid inversion method. *Remote Sensing of Environment*, 165, 123-134. https://doi.org/10.1016/j.rse.2015.04.032

Liu, J., Pattey, E., & Jégo, G. (2012). Assessment of vegetation indices for regional crop green LAI estimation from Landsat images over multiple growing seasons. *Remote Sensing of Environment*, 123, 347-358. https://doi.org/10.1016/j.rse.2012.04.002

Liu, Q., & Huete, A. (1995). A feedback based modification of the NDVI to minimize canopy background and atmospheric noise. *IEEE Transactions on Geoscience and Remote Sensing*, 33(2), 457-465. https://dio.org/10.1109/TGRS.1995.8746027

Liu, X., Guanter, L., Liu, L., Damm, A., Malenovský, Z., Rascher, U. *et al.* (2019). Downscaling of solar-induced chlorophyll fluorescence from canopy level to photosystem level using a random forest model. *Remote Sensing of Environment*, 231, 110772. https://doi.org/10.1016/j.rse.2018.05.035

Ma, B., Li, J., Fan, W., Ren, H., Xu, X., Cui, Y., & Peng, J. (2018). Application of an LAI inversion algorithm based on the unified model of canopy bidirectional reflectance distribution function to the Heihe River Basin. *Journal of Geophysical Research: Atmospheres*, 123(18), 10,671-10,687. https://doi.org/10.1029/2018JD028415

Maccioni, A., Agati, G., & Mazzinghi, P. (2001). New vegetation indices for remote

measurement of chlorophylls based on leaf directional reflectance spectra. *Journal of Photochemistry and Photobiology B: Biology*, 61, 52-61. https://doi.org/10.1016/S1011-1344(01)00145-2

Meerdink, S. K., Hook, S. J., Roberts, D. A., & Abbott, E. A. (2019). The ECOSTRESS spectral library version 1.0. *Remote Sensing of Environment*, 230, 111196. https://doi.org/10.1016/j.rse.2019.05.015

Morcillo-Pallarés, P., Rivera-Caicedo, J. P., Belda, S., Grave C. D., Burriel, H., Moreno, J., & Verrelst, J. (2019). Quantifying the robustness of vegetation indices through global sensitivity analysis of homogeneous and forest leaf-canopy radiative transfer models. *Remote Sensing*, 11, 2418. https://doi.org/10.3390/rs11202418

Mousivand, A., Menenti, M., Gorte, B., & Verhoef, W. (2014). Global sensitivity analysis of the spectral radiance of a soil-vegetation system. *Remote Sensing of Environment*, 145, 131-144. https://doi.org/10.1016/j.rse.2014.01.023

Qi, J., Chehbouni, A., Huete, A. R., Kerr, Y. H., & Sorooshian, S. (1994). A modified soil adjusted vegetation index. *Remote Sensing of Environment*, 48, 119-126. https://doi.org/10.1016/0034-4257(94)90134-1

Quemada, M., & Daughtry, C. S. T. (2016). Spectral indices to improve crop residue cover estimation under varying moisture conditions. *Remote Sensing*, 8, 660. https://doi.org/10.3390/rs8080660

Rahman, M. R., Islam, A. H. M. H., & Rahman, M. A. (2004). NDVI derived sugarcane area identification and crop condition assessment. *Plan Plus*, 1(2), 1-12.

Rondeaux, G., Steven, M., & Baret, F. (1996). Optimization of soil-adjusted vegetation indices. *Remote Sensing of Environment*, 55, 95-107. https://doi.org/10.1016/0034-4257(95)00186-7

Rouse, J. W., Haas, R. H., Schell, J. A., & D.W. (1974). Deering Proceedings of the Third Earth Resources Technology Satellite-1 Symposium, NASA, Greenbelt, MD, pp. 301-317.

Saltelli, A., & Annoni, P. (2010). How to avoid a perfunctory sensitivity analysis. *Environmental Modelling and Software*, 24, 1508-1517. https://doi.org/10.1016/j.envsoft.2010.04.012

Saltelli, A., Annoni, P., Azzini, I., Campolongo, F., Ratto, M., Tarantola, S. (2010). Variance based sensitivity analysis of model output. Design and estimator for the total sensitivity index. *Computer Physics Communications*, 181, 259-270. https://doi.org/10.1016/j.cpc.2009.09.018

Saltelli, A., Ratto, M., Andres, T., Campolongo, F., Cariboni, J., Gatelli, D., Saisana, M., & Tarantola, S. (2008). Global sensitivity analysis: the primer. John Wiley & Sons.

Shabanov, N. V., Knyazikhin, Y., Baret, F., & Myneni, R. B. (2000). Stochastic modeling of radiation regime in discontinuous vegetation canopies. *Remote Sensing of Environment*, 74, 125-144. https://doi.org/10.1016/S0034-4257(00)00128-0

Shi, Z., Wang, Q., Peng, J., Ji, W., Liu, H., Li, X., & Rossel, R. A. V. (2014). Development of a national VNIR soil-spectral library for soil classification and prediction of organic matter concentrations. *Science China Earth Sciences*, 57, 1671-1680. https://doi.org/10.1007/s11430-013-4808-x

SIMLAB (2009). Version 2.2, simulation environment for uncertainty and sensitivity analysis. *Developed by the Joint Research Centre of the European Commission* http://simlab.jrc.ec.euro

Tits, L., Somers, B., Stuckens, J., Farifteh, J., & Coppin, P. (2013). Integration of in situ measured soil status and remotely sensed hyperspectral data to improve plant production system monitoring: Concept, perspectives and limitations. *Remote Sensing of Environment*, 128, 197-211. https://doi.org/10.1016/j.rse.2012.10.006

Van Beek, J., Tits, L., Somers, B., Deckers, T., Janssens, P., & Coppin, P. (2015). Reducing background effects in orchards through spectral vegetation index correction. International Journal of Applied Earth Observation and Geoinformation, 24, 167-177. https://doi.org/10.1016/j.jag.2014.08.009

Verger, A., Vigneau, N., Chéron, C., Gilliot, J. M., Comar, A., Baret, F. (2014). Green area index from an unmanned aerial system over wheat and rapeseed crops. *Remote Sensing of Environment*, 152, 654-664. https://doi.org/10.1016/j.rse.2014.06.006

Verrelst, J., Rivera, J. P., Gitelson, A., Delegido, J., Moreno, J., & Camps-Valls, G. (2016). Spectral band selection for vegetation properties retrieval using Gaussian processes regression. *International Journal of Applied Earth Observation and*

Geoinformation, 52, 554-567. https://doi.org/10.1016/j.jag.2016.07.016

Verrelst, J., Rivera, J. P., van der Tol, C., Magnani, F., Mohammed, G., & Moreno, J. (2015). Global sensitivity analysis of the SCOPE model: What drives simulated canopy-leaving sun-induced fluorescence? *Remote Sensing of Environment*, 166, 8-21. http://dx.doi.org/10.1016/j.rse.2015.06.002

Verrelst, J., Rivera, J. P., Veroustraete, F., Muñoz-Marí, J., Clevers, J. G. P. W., Camps-Valls, G., & Moreno, J. (2015). Experimental Sentinel-2 LAI estimation using parametric, non-parametric and physical retrieval methods – A comparison. *ISPRS Journal of Photogrammetry and Remote Sensing*, 108, 260-272. https://doi.org/10.1016/j.isprsjprs.2015.04.013

Verrelst, J., Sabater, N., Rivera, J. P., Muñoz-Marí, J., Vicent, J., Camps-Valls, G., & Moreno, J. (2016). Emulation of leaf, canopy and atmosphere radiative transfer models for fast global sensitivity analysis. *Remote Sensing*, 8, 673. https://doi.org/10.3390/rs8080673

Verrelst, J., Schaepman, M. E., Malenovský, Z., Clevers, J. G. P. W. (2010). Effects of woody elements on simulated canopy reflectance: Implications for forest chlorophyll content retrieval. *Remote Sensing of Environment*, 114, 647-656. https://doi.org/10.1016/j.rse.2009.11.004

Wang, S., Yang, D., Li, Z., Liu, L., Huang, C., & Zhang, L. (2019). A global sensitivity analysis of commonly used satellite-derived vegetation indices for homogeneour canopies based on model simulation and random forest learning, *Remote Sensing*, 11, 2547. https://doi.org/10.3390/rs11212547

Wu, C., Niu, Z., Tang, Q., & Huang, W. (2008). Estimating chlorophyll content from hyperspectral vegetation indices: Modeling and validation. *Agricultural and Forest Meteorology*, 148, 1230-1241. https://doi.org/10.1016/j.agrformet.2008.03.005

Xiao, Y., Zhao, W., Zhou, D., & Gong, H. (2014). Sensitivity analysis of vegetation reflectance to biochemical and biophysical variables at leaf, canopy, and regional scales. *IEEE Transactions on Geoscience and Remote Sensing*, 52, 4014-4024. https://doi.org/10.1109/TGRS.2013.2278838

Xu, D., An, D., & Guo, X. (2020). The impact of non-photosynthetic vegetation on LAI

estimation by NDVI in mixed grassland. *Remote Sensing*, 12, 1979. https://dio.org/ 10.3390/rs12121979

Xu, J., Meng, J., & Quackenbush, L. J. (2019). Use of remote sensing to predict the optimal harvest date of corn. *Field Crops Research*, 236, 1-13. https://doi.org/10.1016/j.fcr.2019.03.003

Xu, M., Liu, R., Chen, J. M., Liu, Y., Shang, R., Ju, W., *et al.* (2019). Retrieving leaf chlorophyll content using a matrix-based vegetation index combination approach. *Remote Sensing of Environment*, 224, 60-73. https://doi.org/10.1016/j.rse.2019.01.039

Yao, X., Ren, H., Cao, Z., Tian, Y., Cao, W., Zhu, Y., & Cheng, T. (2014). Detecting leaf nitrogen content in wheat with canopy hyperspectrum under different soil backgrounds. *International Journal of Applied Earth Observation and Geoinformation*, 32, 114-124. https://doi.org/10.1016/j.jag.2014.03.014

Yu, K., Lenz-Wiedemann, V., Chen, X., & Bareth, G. (2014). Estimating leaf chlorophyll of barley at different growth stages using spectral indices to reduce soil background and canopy structure effects. *ISPRS Journal of Photogrammetry and Remote Sensing*, 97, 58-77. https://doi.org/10.1016/j.isprsjprs.2014.08.005

Zhang, L., Guo, C. L., Zhao, L. Y., Zhu, Y., Cao, W. X., Tian, Y. C., *et al.* (2016). Estimating wheat yield by integrating the WheatGrow and PROSAIL models. *Field Crops Research*, 192, 55-66. https://doi.org/10.1016/j.fcr.2016.04.014

Appendix A:

Table A. Main variables of PROSAIL in the global sensitivity analysis

Variable	Symbol	Unit	Range	Reference
Leaf structure parameter	N	-	1.0-2.5	Liu et al. (2012)
Leaf chlorophyll content	C_{ab}	$\mu g/cm^2$	5-100	Xu et al. (2019)
Leaf carotenoid content	C_{xc}	$\mu g/cm^2$	8	Liang et al. (2015)
Brown pigment content	C_{bp}	-	0	Xu et al. (2019)
Equivalent water thickness	C_w	cm	0.0043-0.0713	Feret et al. (2011)
Dry matter content	C_m	g/cm^2	0.0008-0.0331	Feret et al. (2011)
Leaf area index	LAI	m^2/m^2	0.1-10	Liang et al. (2015)
Average leaf inclination angle	ALA	°	30-80	Verger et al. (2014)
Hot-spot parameter	S_L	-	0.2	Xiao et al. (2014)
Background brightness factor	α	-	0-1	Verrelst et al. (2015)
Solar zenith angle	θ_s	°	20-60	-
Viewing zenith angle	θ_v	°	0	-
Relative azimuth angle	φ_{sv}	°	0	-
Ratio of diffuse to total incident radiation	*skyl*	%	10	Zhang et al. (2016)

Note: a uniform distribution was assigned to these variables.

Appendix B:

A reasonable sample size of input parameters is crucial not only for the accuracy of the sensitivity analysis but also to ensure the feasibility and a reasonable computational cost of the simulation. To assess how sample size affects the convergence of the sensitivity indices, we ran a set of the EFAST global sensitivity analysis with gradually increasing sample size and then computed the total-order sensitivity index of the widely-used NDVI based on the narrowband reflectance at 670 and 800 nm from PROSAIL simulations, corresponding to eight variables. The result indicates that about 30 000 samples suffice to distinguish between influential and noninfluential parameters. Specifically, no more fluctuations occur after 40 000 simulations. Thus, a total of 40 000 combinations of model parameters (N, C_{ab}, C_w, C_m, LAI, ALA, α, θ_s) are randomly generated with the EFAST. This set of random samples is then used with each background reflectance to simulate the canopy reflectance and to analyze the sensitivity.

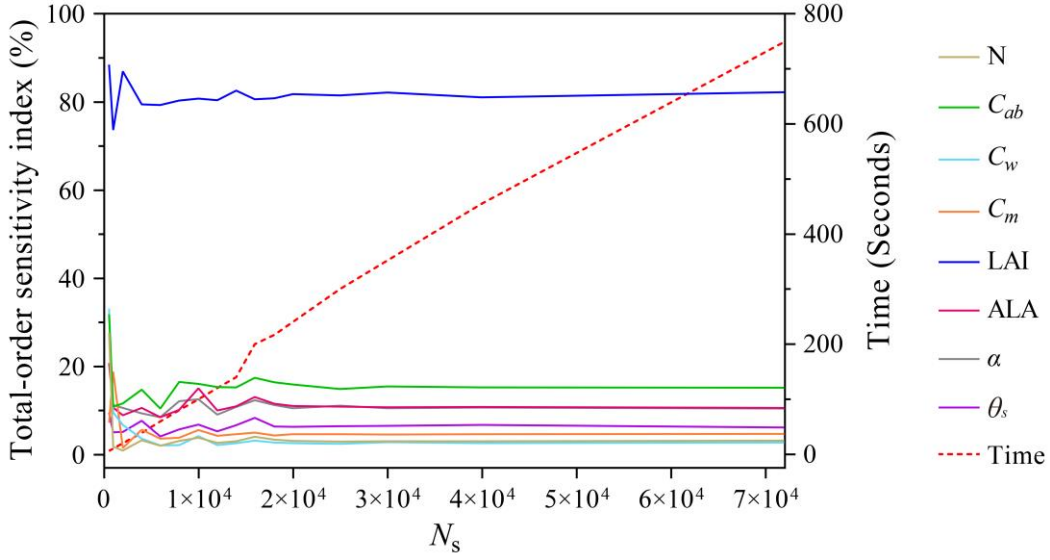


Figure A. Analysis of the impact of total number of samples (N_s) on the stability of global sensitivity analysis for NDVI with PROSAIL based on the extended Fourier amplitude sensitivity test.

Appendix C:

Table B. A set of vegetation indices examined in this paper

Spectral index	Formulation	Estimation or Elimination	Reference
MSAVI, Modified soil adjusted vegetation index	$0.5\left[2R_{800}+1-\sqrt{(2R_{800}+1)^2-8(R_{800}-R_{670})}\right]$	Background effect	Qi et al. (1994)
OSAVI, Optimized soil adjusted vegetation index	$(1+0.16)\,(R_{800}-R_{670})/(R_{800}+R_{670}+0.16)$	Background effect	Rondeaux et al. (1996)
NDVI, Normalized difference vegetation index	$(R_{800}-R_{670})/(R_{800}+R_{670})$	LAI	Rouse et al. (1974)
MSR, Modified simple ratio	$[(R_{800}/R_{670})-1]/\sqrt{(R_{800}/R_{670})+1}$	LAI	Chen (1996)
MCARI2, Modified chlorophyll absorption ratio index 2	$\frac{1.5[2.5(R_{800}-R_{670})-1.3(R_{800}-R_{550})]}{\sqrt{(2R_{800}+1)^2-\left(6R_{800}-5\sqrt{R_{670}}\right)-0.5}}$	LAI	Haboudane et al. (2004)
sLAIDI, Standardized LAI Determining Index	S $(R_{1050}-R_{1250})/(R_{1050}+R_{1250})$, where S = 5	LAI	Delalieux et al. (2008)
CI_{RE}, Red-edge chlorophyll index	$(R_{750}/R_{710})-1$	Chlorophyll	Gitelson et al. (2006)
MTCI, MERIS terrestrial chlorophyll index	$(R_{754}-R_{709})/(R_{709}-R_{681})$	Chlorophyll	Dash and Curran (2004)
Macc01, Maccioni index	$(R_{780}-R_{710})/(R_{780}-R_{680})$	Chlorophyll	Maccioni et al. (2001)
LICI, LAI-insensitive chlorophyll index	$(R_{735}/R_{720})-[(R_{573}-R_{680})/(R_{573}+R_{680})]$	Chlorophyll	Li et al. (2020)
$MCARI_{(705,\,750)}/OSAVI_{(705,\,750)}$	$\frac{[(R_{750}-R_{705})-0.2(R_{750}-R_{550})]\left(\frac{R_{750}}{R_{705}}\right)}{\left[\frac{(1+0.16)(R_{750}-R_{705})}{R_{750}+R_{705}+0.16}\right]}$	Chlorophyll	Wu et al. (2008)

PRI, Photochemical reflectance index	$(R_{531} - R_{570})/(R_{531} + R_{570})$	Photosynthetic efficiency	Gamon et al. (1992)